

FILE COPY

AD E 951 609

(1)

TECHNICAL REPORT RD-RE-90-6

AD-A232 117

EVALUATION OF A FERROELECTRIC LIQUID CRYSTAL
SPATIAL LIGHT MODULATOR

T. D. Hudson
R. Kevin Worcester
Don A. Gregory
Weapons Sciences Directorate
Research, Development, and Engineering
Center

JANUARY 1991

DTIC
ELECTE
MAR 15 1991
S D



U.S. ARMY MISSILE COMMAND

Redstone Arsenal, Alabama 35898-5000

Approved for public release; distribution is unlimited.

DESTRUCTION NOTICE

**FOR CLASSIFIED DOCUMENTS, FOLLOW THE PROCEDURES IN
DoD 5200.22-M, INDUSTRIAL SECURITY MANUAL, SECTION
II-19 OR DoD 5200.1-R, INFORMATION SECURITY PROGRAM
REGULATION, CHAPTER IX. FOR UNCLASSIFIED, LIMITED
DOCUMENTS, DESTROY BY ANY METHOD THAT WILL PREVENT
DISCLOSURE OF CONTENTS OR RECONSTRUCTION OF THE
DOCUMENT.**

DISCLAIMER

**THE FINDINGS IN THIS REPORT ARE NOT TO BE CONSTRUED
AS AN OFFICIAL DEPARTMENT OF THE ARMY POSITION
UNLESS SO DESIGNATED BY OTHER AUTHORIZED DOCUMENTS.**

TRADE NAMES

**USE OF TRADE NAMES OR MANUFACTURERS IN THIS REPORT
DOES NOT CONSTITUTE AN OFFICIAL ENDORSEMENT OR
APPROVAL OF THE USE OF SUCH COMMERCIAL HARDWARE OR
SOFTWARE.**

UNCLASSIFIED
SECURITY CLASSIFICATION OF THIS PAGE

Form Approved
OMB No 0704-0188
Exp Date Jun 30 1986

REPORT DOCUMENTATION PAGE

1. REPORT SECURITY CLASSIFICATION UNCLASSIFIED		1b RESTRICTIVE MARKINGS	
2. SECURITY CLASSIFICATION AUTHORITY		3. DISTRIBUTION/AVAILABILITY OF REPORT Approved for public release; distribution unlimited	
4. DECLASSIFICATION/DOWNGRADING SCHEDULE		5. MONITORING ORGANIZATION REPORT NUMBER(S)	
PERFORMING ORGANIZATION REPORT NUMBER(S) R-RD-RE-90-6		6b OFFICE SYMBOL (If applicable) AMSMI-RD-WS	
7. NAME OF PERFORMING ORGANIZATION Weapons Sciences Directorate D&E Center		7a NAME OF MONITORING ORGANIZATION	
8. ADDRESS (City, State, and ZIP Code) Commander J.S. Army Missile Command ATTN: AMSMI-RD-RE, Redstone Arsenal, AL 35898-5248		7b ADDRESS (City, State, and ZIP Code)	
9. NAME OF FUNDING/SPONSORING ORGANIZATION		8b OFFICE SYMBOL (If applicable)	
10. ADDRESS (City, State, and ZIP Code)		9. PROCUREMENT INSTRUMENT IDENTIFICATION NUMBER	
		10. SOURCE OF FUNDING NUMBERS	
		PROGRAM ELEMENT NO.	PROJECT NO.
		TASK NO.	WORK UNIT ACCESSION NO.
1. TITLE (Include Security Classification) Evaluation of a Ferroelectric Liquid Crystal Spatial Light Modulator			
2. PERSONAL AUTHOR(S) Tracy D. Hudson			
3a. TYPE OF REPORT Final	13b. TIME COVERED FROM _____ TO _____	14. DATE OF REPORT (Year, Month, Day) 1991/Jan/9	15. PAGE COUNT 31
6. SUPPLEMENTARY NOTATION			
7. COSATI CODES		18. SUBJECT TERMS (Continue on reverse if necessary and identify by block number) Optical Pattern Recognition Spatial Light Modulator Optical Computing	
9. ABSTRACT (Continue on reverse if necessary and identify by block number) Key performance characteristics of an optically-addressed ferroelectric liquid crystal spatial light modulator have been measured and compare favorably with other commercially available SLMs. Several characteristics which are important for optical pattern recognition, including imaging resolution, visibility, and response time, are discussed in this communication. The maximum resolution was measured to be 40 lp/mm with an imaging response time of 60 Hz. This differs substantially from previously published results. This is primarily due to operating the device so as to maintain good resolution with moderate illumination. Furthermore, experimental results to determine the modulated response of the read beam as a function of the write light intensity will also be presented.			
20. DISTRIBUTION/AVAILABILITY OF ABSTRACT <input type="checkbox"/> UNCLASSIFIED/UNLIMITED <input checked="" type="checkbox"/> SAME AS RPT <input type="checkbox"/> DTIC USERS		21. ABSTRACT SECURITY CLASSIFICATION UNCLASSIFIED	
22a. NAME OF RESPONSIBLE INDIVIDUAL Tracy D. Hudson		22b. TELEPHONE (Include Area Code) (205) 876-7687	22c. OFFICE SYMBOL AMSMI-RD-WS-PO
23. FORM 1473, 84 MAR		83 APR edition may be used until exhausted All other editions are obsolete	
		SECURITY CLASSIFICATION OF THIS PAGE UNCLASSIFIED	

CONTENTS

	<u>Page</u>
I. INTRODUCTION.....	1
II. DEVICE CONSTRUCTION.....	1
III. RESOLUTION MEASUREMENTS.....	2
IV. VISIBILITY MEASUREMENTS.....	3
V. IMAGING RESPONSE MEASUREMENTS.....	5
VI. MODULATION RESPONSE OF READ BEAM AS A FUNCTION OF WRITE LIGHT INTENSITY.....	7
VII. CONCLUSIONS.....	8

Accesion For	
NTIS CRA&I	<input checked="" type="checkbox"/>
DTIC TAB	<input type="checkbox"/>
Unannounced	<input type="checkbox"/>
Justification	
By _____	
Distribution / _____	
Availability Codes	
Dist	Avail and/or Special
A-1	



LIST OF ILLUSTRATIONS

<u>Figure</u>	<u>Title</u>	<u>Page</u>
1	Schematic representation of the optically-addressed ferroelectric spatial light modulator.....	12
2	Optical system implemented to measure the maximum resolution of the ferroelectric LC SLM.....	13
3	Resolution of the optically-addressed FELC SLM.....	14
4	Optical system implemented to measure the visibility of the ferroelectric LC SLM.....	15
5	Modulation Transfer Function (MTF) of (a) the optical system shown in Figure 4 with and without the FELC SLM present; and (b) the FELC modulator alone.....	16
6	Experimental system used to measure the response time of the ferroelectric LC SLM.....	17
7	Graphical representation of the modulator's response in the experimental system of Figure 6.....	18
8	Spatial light modulator response using a low-pass analog filter to attenuate the high frequency modulation shown in Figure 7.....	18
9	The (a) rise and (b) fall time of the optically addressed FELC modulator.....	19
10	Experimental system used to measure the response of the FELC SLM to variations in write light intensity.	20
11	The response of the FELC SLM to variations in write light intensity when the modulator was operated in a (a) "maximum contrast" or (b) "phase-only" mode.....	21

ACKNOWLEDGEMENTS

The authors express their grateful appreciation to Garret Moddel and Bruce Landreth of the University of Colorado - Boulder for their assistance in explaining the physical mechanisms involved in operating the FELC device and to David J. Lanteigne of the Research Directorate, U.S. Army Missile Command for his explanation of the FELC SLM acting as a thin phase grating. The authors are also thankful for the assistance of Ms. Cindy Gabardi in preparing this manuscript.

I. INTRODUCTION

A major technological hurdle for optical computing and optical pattern recognition is the current state of performance of spatial light modulators (SLM's). The slow response, low resolution, and poor visibility of spatial light modulators have significantly limited their application in optical computing and pattern recognition.

Progress in spatial light modulator technology has been forthcoming over the past few years. Performance characteristics, such as response time, resolution, and visibility, have been steadily improving in SLM's. Some commonly considered SLM's for pattern recognition purposes include magneto-optic SLM's[2], deformable mirror devices[3], microchannel SLM's[4], and ferroelectric LC devices[1,5-6]. This communication discusses the performance characterizations of the newest of these SLM's - optically addressed ferroelectric LC devices.

II. DEVICE CONSTRUCTION

The basic construction and theory of operation of the optically-addressed ferroelectric liquid crystal (FELC) SLM, fabricated by the University of Colorado - Boulder and displaytech, Inc., is similar to the Hughes LCLV[7]. A sketch of the FELC device is shown in Figure 1. Hydrogenated amorphous silicon is used as the photosensor and the ferroelectric liquid crystal (SCE9)[8] is smectic C*. Typical operation of the FELC SLM requires the application of a 17V peak-to-peak amplitude of a 1.5 KHz square wave with a 2V DC offset.

The laboratory grade device did not have dielectric coatings nor use optical flats for the sandwich structure. The absence of the dielectric coatings allowed for the unwanted transmission of the write beam through the liquid crystal. A great deal of unmodulated light was transmitted by the device when it was addressed using broadband white light. Experimentally, it was found that green light was well absorbed while still providing enough activation energy for the amorphous silicon photosensor. The device was operated with an incident write light of $300 \mu\text{W}/\text{cm}^2$ intensity and 514.4 nm wavelength. This intensity corresponds to the lower limits of the device, capable of operating between 0.2 and $60 \text{ mW}/\text{cm}^2$ write light intensity. The reflectivity of the FELC SLM was also limited by the absence of a dielectric mirror to be 23%.

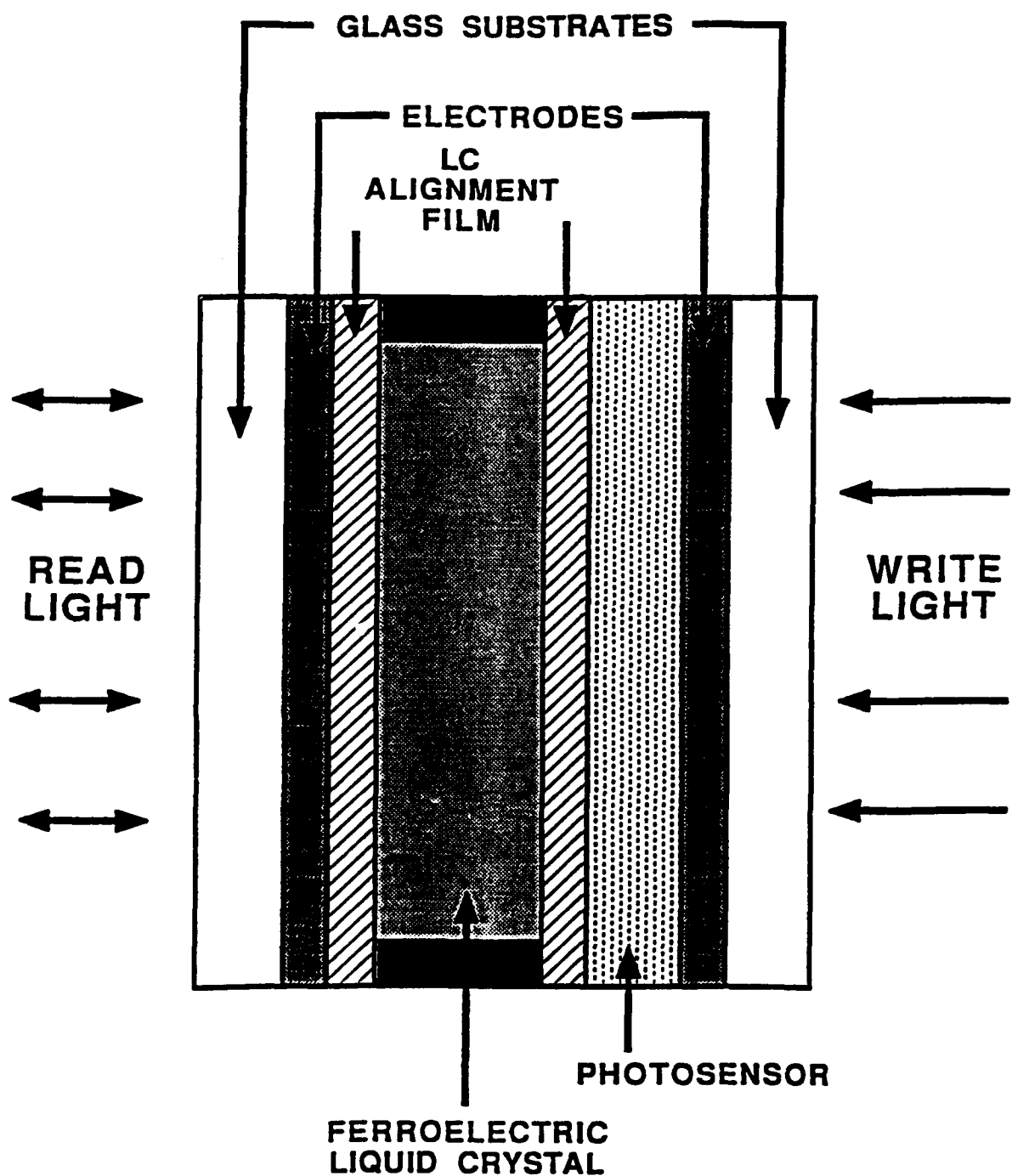


Figure 1. Schematic representation of the optically-addressed ferroelectric liquid crystal spatial light modulator.

III. RESOLUTION MEASUREMENTS

The resolution of the ferroelectric SLM was measured using the optical system depicted in Figure 2. A USAF resolution transparency was imaged 1:1 on the write side of the FELC SLM using a 50 mm focal length imaging lens (54 mm dia.) and a collimated beam of light provided by an Argon laser. The read beam, spatially filtered and collimated using standard laboratory techniques, was provided by a HeNe laser source ($\lambda=632.8$ nm). Lens L2, a 192 mm focal length bi-convex doublet (54 mm dia.), was used to image the modulated light from the FELC SLM onto the CCD camera. The location of this lens was chosen so that a 2:1 imaging ratio occurred between the modulator and the camera. The polarizer and half-wave plate were adjusted for maximum image visibility at the CCD plane. The transmission of any write light ($\lambda=514.5$ nm) through the device was immeasurable at the CCD plane.

Figure 3 is a photograph of the resolution chart's image at the CCD plane. This photo was taken from a monitor connected to the camera. The least resolvable order is the third element in group 5. The resolution of this element corresponds to 40.3 lp/mm. The resolution measurement techniques and results compare favorably to previously published results [1,9]. The modulator was temporarily replaced with the USAF resolution chart, a "chrome-on-glass" transparency, to verify that any optical components or the CCD were not the limitation to this resolution. The least resolvable order corresponded to >50 lp/mm for this arrangement. Therefore, the maximum imaging resolution of the FELC device was determined to be 40.3 lp/mm. A photo-detector was then inserted to determine the corresponding write light incident on the modulator to achieve this resolution. The write light intensity was measured to be $260 \mu\text{W}/\text{cm}^2$ at the FELC write plane. The read light, though not as important, was measured to be $55 \mu\text{W}/\text{cm}^2$ at the FELC read plane.

Other researchers have obtained higher values for the spatial resolution of ferroelectric liquid crystal spatial light modulators by using a pair of coherent beams to write a holographic interference pattern on the write side of the device, and observing the far-field diffraction pattern of the reflected read beam.* Multiple orders of diffraction are usually observed. It has been assumed that the binary response of the smectic C* ferroelectric liquid crystals maps the incident sinusoidal fringe pattern into a square wave output. Therefore, each diffraction order was taken to present one harmonic component of the Fourier decomposition of a square wave. The highest observed diffraction order then gave the highest spatial frequency resolved on the device, as an integral multiple of the spatial frequency of the incident pattern.

* Personal communication with Dr. Garret Moddel, Electrical and Computer Engineering Dept. and Optoelectronics Computing Systems Center, University of Colorado - Boulder, Boulder, CO 80309.

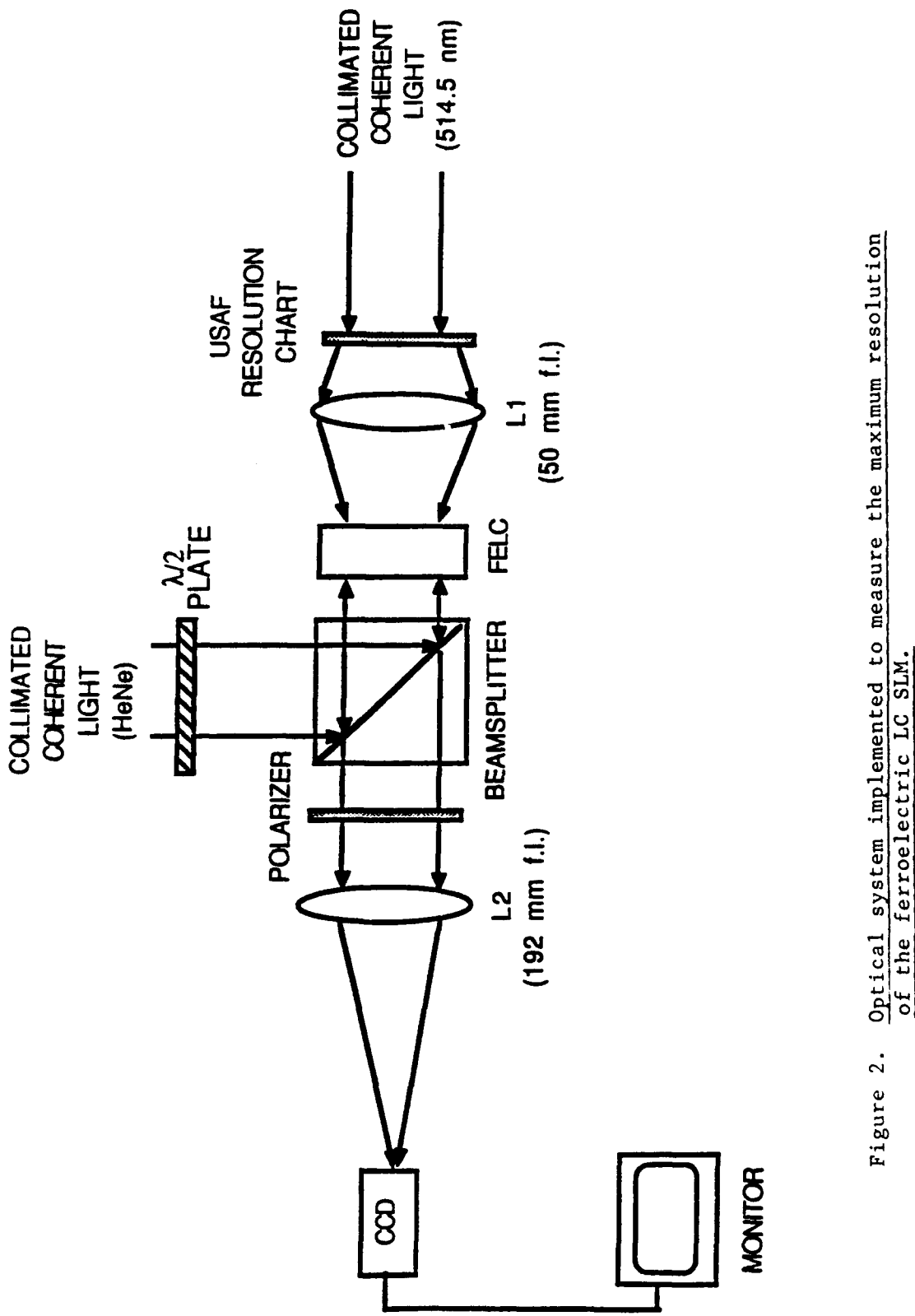


Figure 2. Optical system implemented to measure the maximum resolution of the ferroelectric LC SLM.

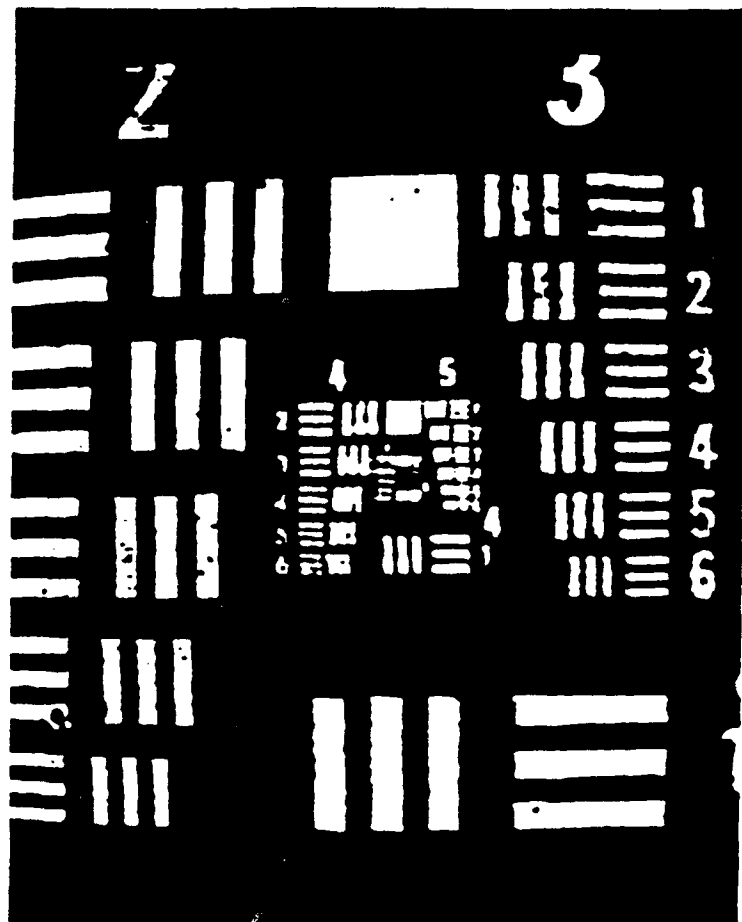


Figure 3. Resolution of the optically-addressed FELC SLM. Resolved the Group 5, Element 3 order which corresponded to 40.3 1p/mm.

However, the extraction of spatial frequency information from the diffraction pattern of the read beam is problematic, since, for spatial frequencies of interest, the FELC SLM acts as a thin phase grating; i.e., it operates in the Raman-Nath regime. A grating is normally considered to be "thin" when the following condition is met[10]:

$$(d\lambda/\Lambda^2) \ll 1 \quad (1)$$

For typical parameters of liquid crystal grating layer thickness ($d = 3 \mu\text{m}$), HeNe read beam ($\lambda = 632.8 \text{ nm}$), and incident sinusoidal interference pattern period ($\Lambda = 25 \mu\text{m}$ for a 40 lp/mm input pattern), the thin grating condition is easily met, even though the grating is several wavelengths thick.

The most striking characteristics of a sinusoidal thin phase grating is that it exhibits multiple diffraction orders even if there is only one spatial frequency component in the grating. Obviously, linear superposition still holds, and higher harmonics in the grating will contribute to the diffraction pattern, but the presence of higher order diffraction modes from a thin grating is not sufficient proof of higher spatial frequencies in the grating.

IV. VISIBILITY MEASUREMENTS

Visibility is a measure of the quality of an image produced by a system. Following Michelson[11], visibility is defined as

$$v = \frac{I_{\max} - I_{\min}}{I_{\max} + I_{\min}} \quad (2)$$

where I_{\max} and I_{\min} are the maximum and minimum intensities of the resulting image. The optical system shown in Figure 4 was implemented to measure the visibility of the FELC modulator. Initially a totally dark vs. a totally bright image was written to the modulator with a photodetector located at the imaging plane P. The variation in the energy measured in plane P corresponded to a visibility of 0.90.

The visibility of the optically-addressed FELC modulator will improve with the use of optical flats, instead of glass plates, for the sandwich structure. The glass plates of the laboratory grade modulator created an interference pattern of Newton's rings in the image plane. These rings increased the average of the background noise thus increasing the value of I_{\min} observed with the photodetector. The visibility of the signal detected by the photodetector may also be reduced by sufficiently intense read beam illumination. The read beam was attenuated well below the saturation level of the detector to negate this effect.

The USAF resolution transparency was then reimaged 1:1 on the modulator. The photodetector in plane P was replaced with a Pulnix TM-540 CCD camera and lens L2, a 254 mm f.1. biconvex lens (54 mm dia), was located so that a 1:1 imaging occurred between the modulator and camera. The video output of the camera was channeled to a video analyzer and chart recorder. The video analyzer/chart recorder allowed for the scanning of a horizontal or vertical line of video across the modulator's image of the resolution chart.

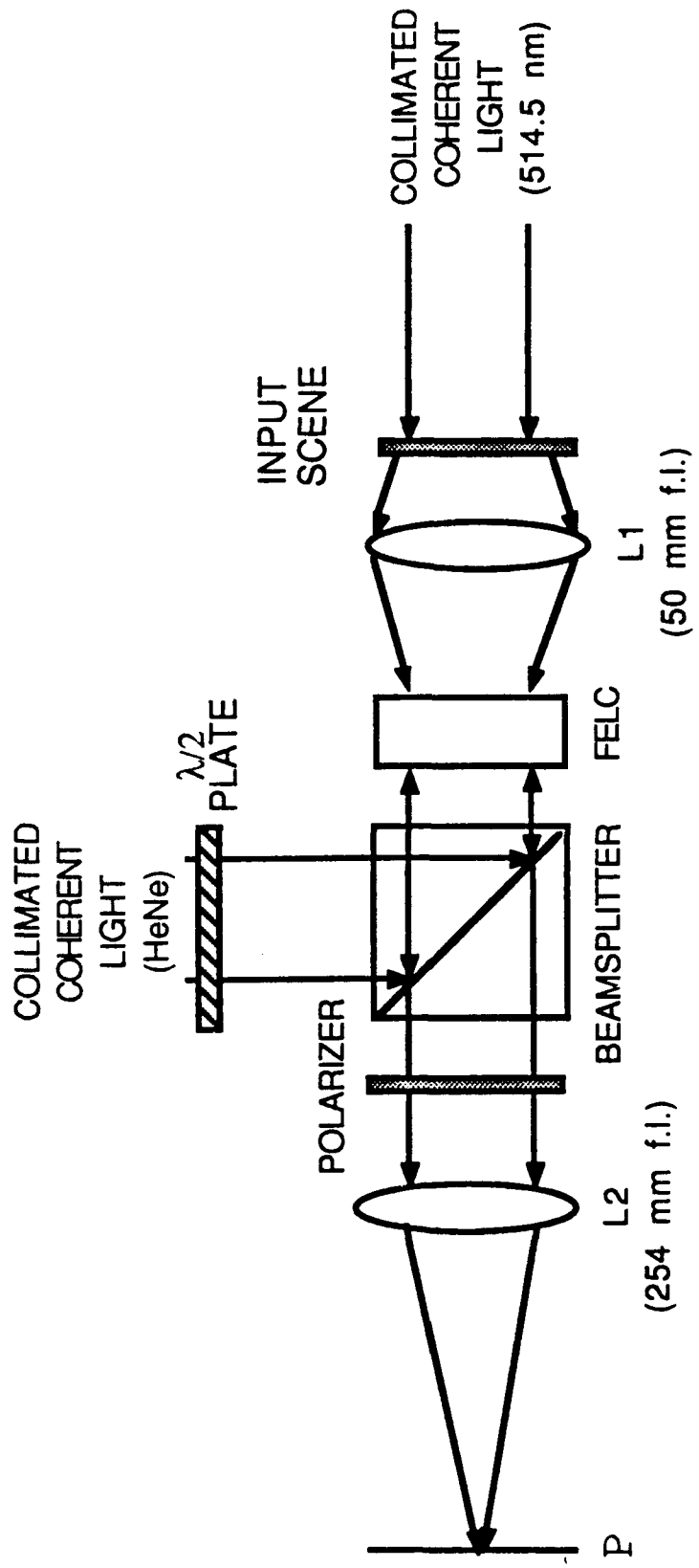


Figure 4. Optical system implemented to measure the visibility of the ferroelectric SLM.

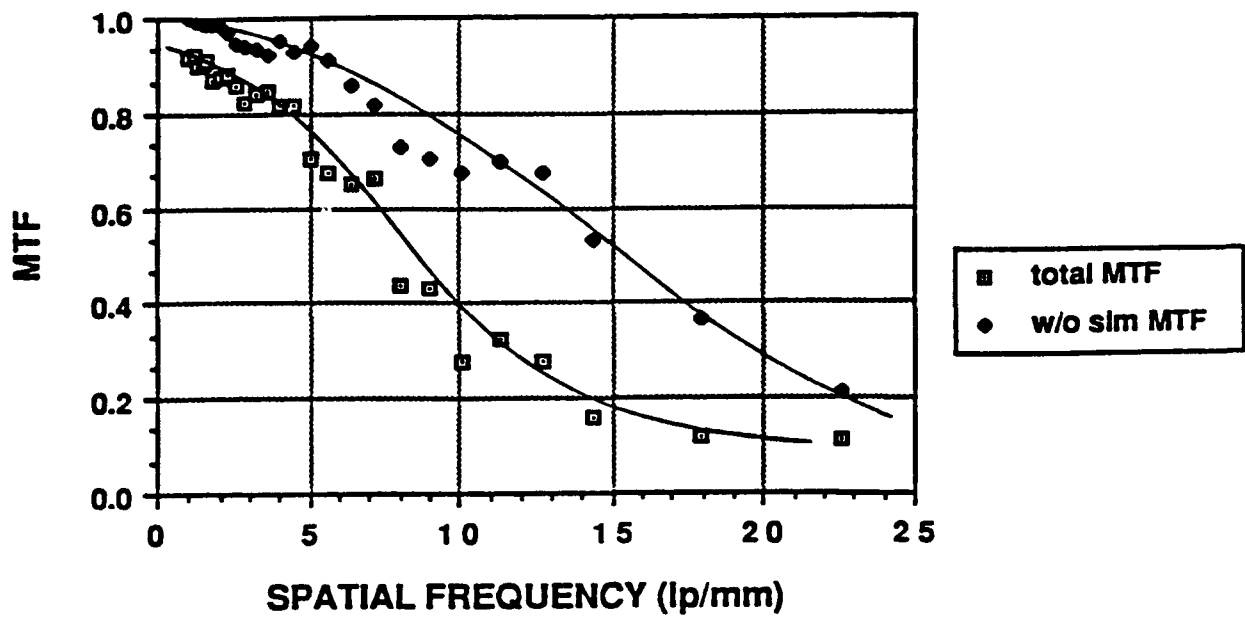
Video traces across each resolvable set of bars comprising the groups and elements of the chart were performed. These traces corresponded to a measurement of the visibility for varying spatial frequencies. This data essentially comprises a Contrast Transfer Function (CTF) of the optical system. The CTF is a measure of the amplitude response of a system to varying square-wave spatial frequency inputs.[12] However, CTF's of subsystems cannot be cascaded to evaluate the performance of an overall system.

The Modulation Transfer Function (MTF) is a quantitative measure of image quality. The MTF describes the ability of a lens or optical system, as a function of spatial frequency, to transfer an object visibility to the image. The MTF is the amplitude response of a system to varying sine-wave spatial frequency inputs. Furthermore, MTF's permit the cascading of the effects of subsystems in determining the performance of an overall system. The CTF and MTF responses of a lens or system are related by [13]:

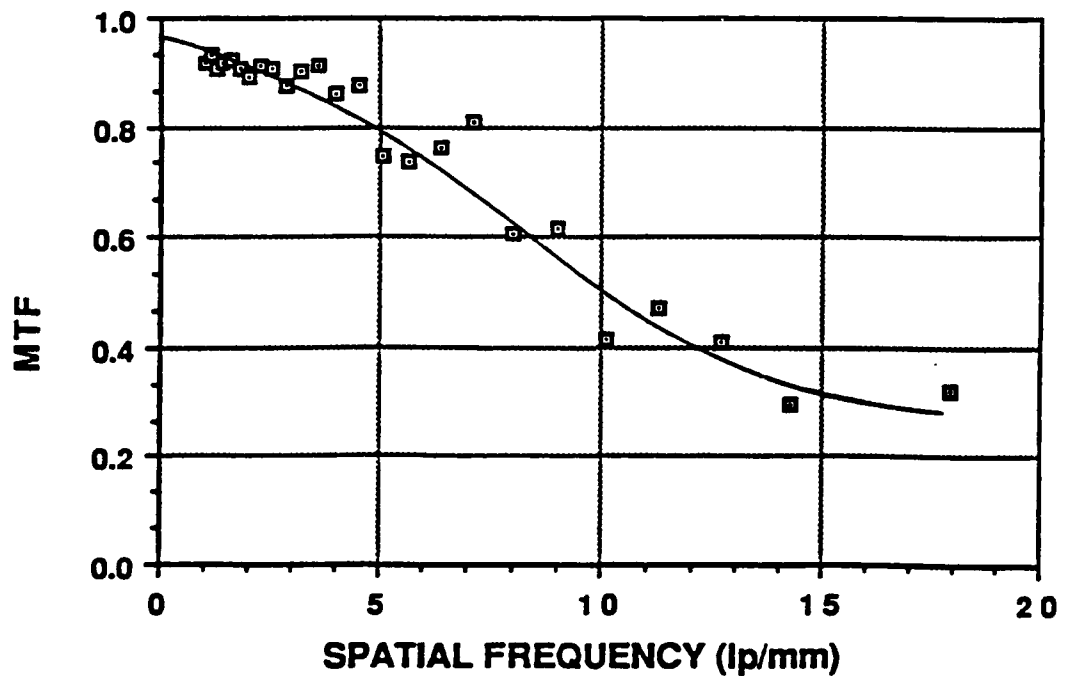
$$MTF = M(f) = [\pi/4] \{C(f) + C(3f)/3 - C(5f)/5 + C(7f)/7 \dots\} \quad (3)$$

where f is the spatial frequency and $C(f)$ is the visibility measured for a known spatial frequency.

The CTF of the system shown in Figure 4 was measured using the video analyzer/chart recorder described above. This CTF includes the effects of the modulator, camera, and the intermediate optical components. Equation (3) was used to determine the MTF of the system. Only the first four terms in the series expansion was used which corresponded to the collection of approximately 98% of the energy arriving at the optical system. The remaining energy is modulated at higher harmonic frequencies of the bar chart fundamental frequency. The resulting MTF is shown in Figure 5a. This MTF curve should not be interpreted as the MTF of the modulator alone. The MTF of the camera and intermediate optics must be removed from this curve to determine the MTF of the FELC device. The FELC device was replaced with the "chrome-on-glass" transparency of the USAF resolution chart. This transparency served as a high resolution test input to the system shown in Figure 4. The video analyzer and chart recorder were again utilized using the techniques described above to measure the CTF. The MTF was calculated from this CTF and is also shown in Figure 5a. The MTF of the SLM was determined by dividing the total MTF by the optical system MTF. The results are shown in Figure 5b. The curves shown in Figure 5 are empirical "best-fit" approximations to the data.



(a)



(b)

Figure 5. Modulation Transfer Function (MTF) of (a) the optical system shown in Figure 4 with and without the FELC SLM present, and (b) the FELC modulator alone.

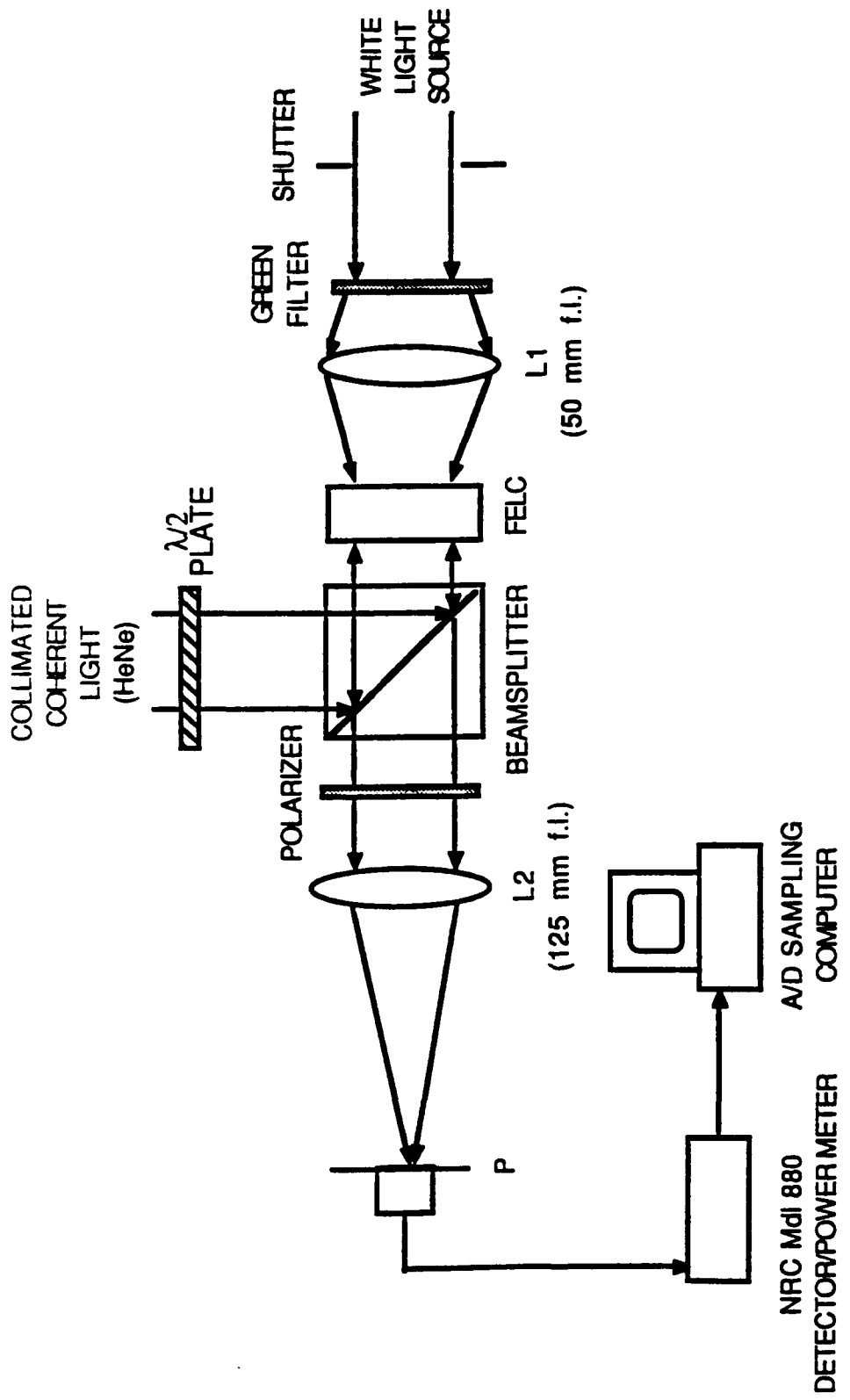
V. IMAGING RESPONSE MEASUREMENTS

The response time of the ferroelectric LC SLM was measured using the optical system shown in Figure 6. This experimental system differs from the systems used above to measure the resolution and visibility. The response time experiment utilized a broadband white light source for the write beam illumination. A green band-pass filter was used in conjunction with this source but a significant amount of near-IR light was transmitted through this filter and consequently through the ferroelectric liquid crystal layer. An electronic shutter was used to cycle the write beam "on" or "off" on the modulator. The polarizer and half-wave plate shown in the read beam were adjusted for maximum image visibility at plane P. A photo-detector was positioned at P with the output of the detector sampled by an A/D acquisition board located inside a 80286 microprocessor-based computer.

Prior to collection of data from this system, the response limitation of the shutter, detector, and A/D acquisition was determined. The detector was positioned in front of the shutter of the write beam, which was cycled open and closed every 40 milliseconds. The A/D board sampled the output of the detector every 0.2 milliseconds during this cycling. The rise and fall times were determined to be approximately 1 millisecond each for the shutter/detector combination. Therefore, the detector, shutter, and A/D acquisition process should not limit the response measurement of the modulator until approximately 500 Hz.

Figure 7 is a plot of the modulator response from the optical system shown in Figure 6. The shutter was cycled open and closed at a 25 Hz frequency. The high frequency modulation on the response curve is due to the device being driven by a 1.5 kHz square wave voltage. The reason that the output of the device oscillates at this frequency is that the device is at least partially erased during the forward-bias portion of the square wave cycle. Ideally, the device would be completely erased during every forward bias period but the photoconductive effects of the amorphous silicon photo-sensor presently limits this response. The large amplitude of this high frequency modulation obscured the rise and fall times of the optical response. Analog filtering was employed prior to the A/D sampling to more clearly determine the optical response of writing to the modulator vs the electrical response due to the driving frequency of the device. Several low-pass filters were utilized. The cutoff frequency of these filters included 500, 200, and 100 Hz. Comparison of the resulting response curves with these varying filters revealed no characteristic change in the shape of the optical response while successfully suppressing most of the high frequency modulation.

Figure 8 shows the optical response of the ferroelectric liquid crystal modulator using a low-pass analog filter with a 100 Hz cutoff frequency. Figure 9(a) and 9(b) are magnified portions of the response curve emphasizing rise and fall times respectively. The rise time, measured from the baseline to the maximum value, was 10.0 milliseconds. The fall time, from maximum value to the baseline, was 7.3 milliseconds. The cycle time is 17.3 milliseconds which corresponds to approximately 60 Hz. This response was taken near the optimal visibility of the modulator with approximately 0.6 mW/cm^2 incident on the write side of the device and includes any photoconductive



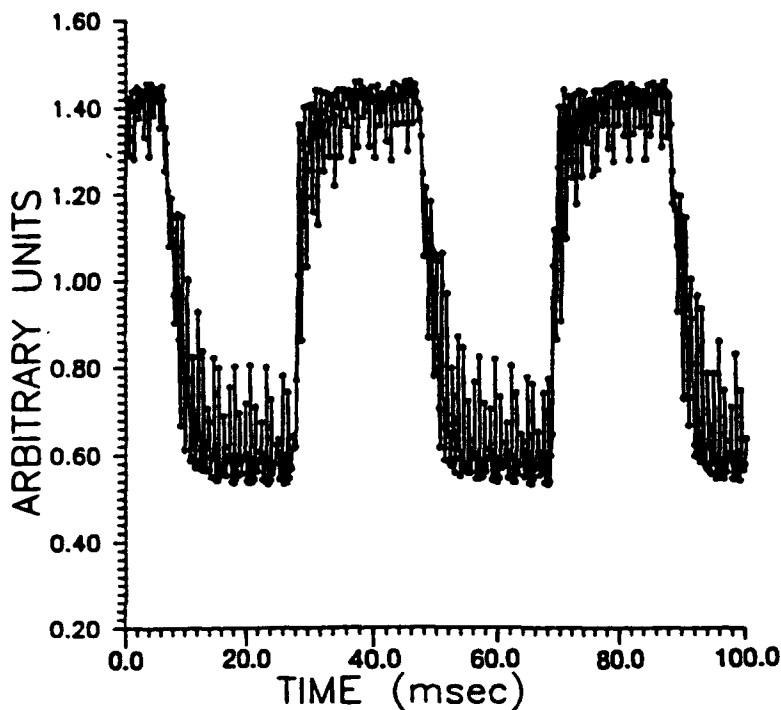


Figure 7. Graphical representation of the modulator's response in the experimental system of Figure 6.

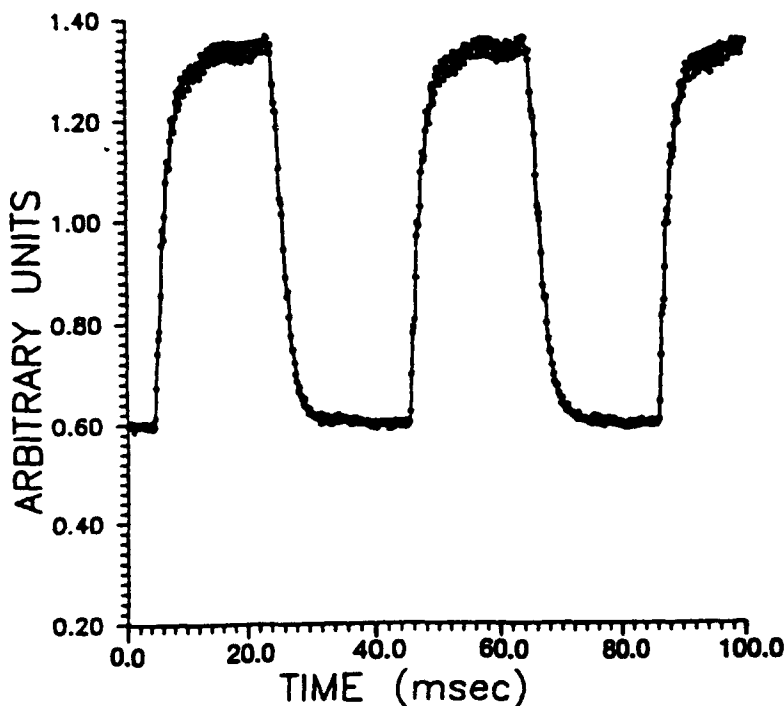
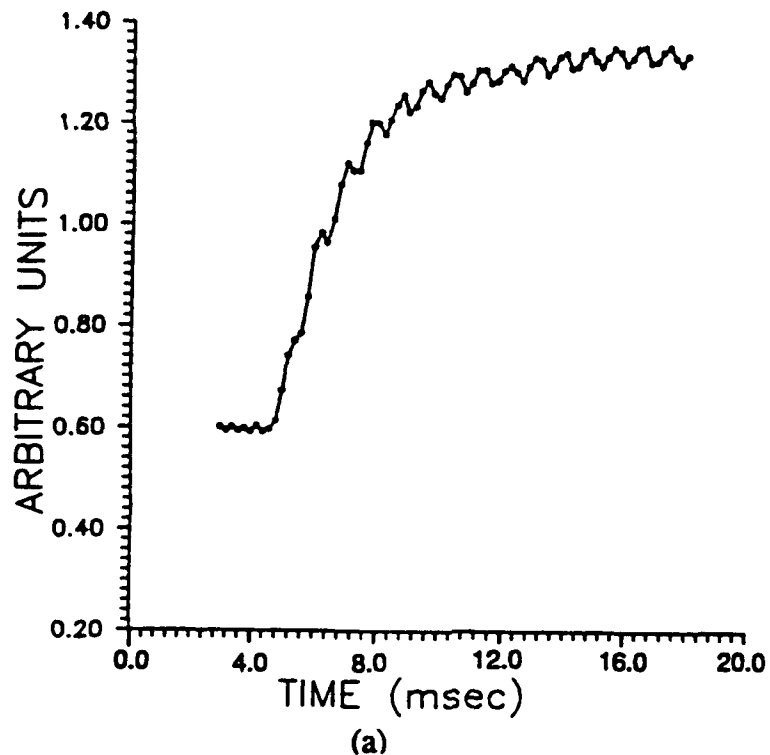
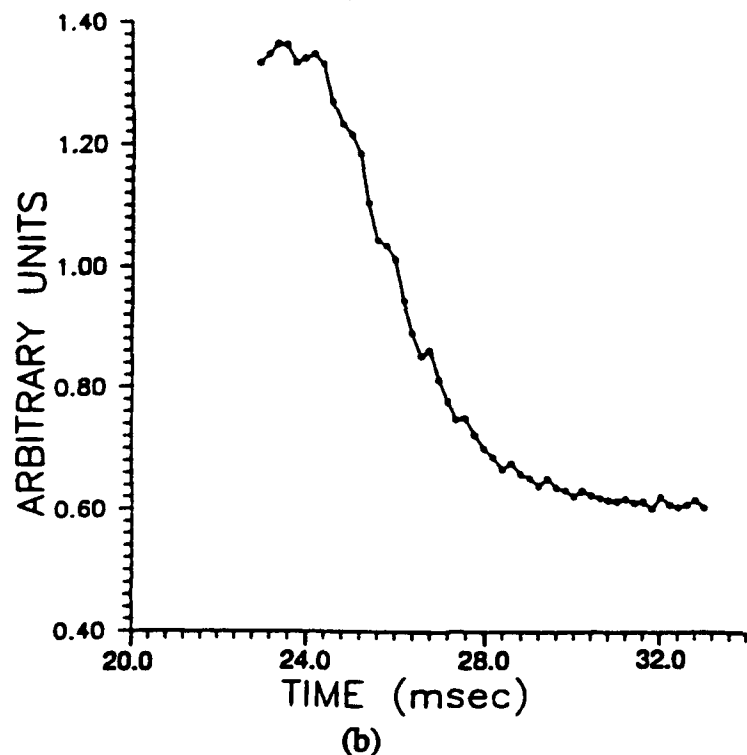


Figure 8. Spatial light modulator response using a low-pass analog filter to attenuate the high frequency modulation shown in Figure 7.



(a)



(b)

Figure 9. Magnified portions of Figure 8 emphasizing the (a) rise and (b) fall times of the optically addressed ferroelectric modulator.

effects due to the properties of the photosensor. This response time differs from previously published research¹¹ which sacrificed maximum visibility and low write light intensities for orders of magnitude increases in response.

Response time is also measured as a function of 10%-90% rise and 90%-10% fall from maximum to minimum read-out intensity. This device has a corresponding 10%-90% rise time of 4.6 msec and 90%-10% fall time of 3.8 msec for a cycle time of 8.4 msec or approximately 120 Hz. However, this response does not occur at optimum visibility.

The optical response of the modulator was also measured as a function of the write light intensity by inserting various neutral density filters in the write beam and repeating the above experiment. For write light intensities varying between 0.1 and 0.6 mW/cm², the rise time increased with decreasing intensity and conversely the fall time decreased with decreasing intensity. The cumulative effect of the rise and fall times resulted in the cycle time remaining constant throughout this range. The rise time decreases with increasing write light intensity because the rate at which the FELC is charged negatively during the (reverse biased) write period is proportional to the write light intensity. As photons are absorbed in the hydrogenated amorphous silicon, mobile charge carriers are created which polarize the FELC. Therefore, the FELC charges faster if the write light is brighter. The reason that the fall time increases with increasing write light intensity is that there is more charge to remove from the FELC before the voltage becomes positive again and the device is erased. Since erasing occurs under forward bias, the rate at which the FELC is discharged is independent of write light intensity. Therefore, when the FELC is charged more negatively during the write period (as it is with brighter write light), it takes longer to discharge during the erase period.

Another commonly quoted measure of response time is the decay constant. The decay constant is the time to rise and fall to within 1/e (63%) of its equilibrium value. Using this definition, the decay constant of the optically-addressed FELC modulator was measured as approximately 9 milliseconds. The decay constant of several liquid crystal televisions which have been used for optical processing have recently been measured and were found to vary between 37 and 150 milliseconds at optimal image visibility.[14]

VI. MODULATION RESPONSE OF READ BEAM AS A FUNCTION OF WRITE LIGHT INTENSITY

Recently, the effect of a nonlinear matched filter in optical correlator architectures has been investigated.[15-19] The operation has been computer simulated for both joint transform and classical matched filter correlators. The nonlinearity of most spatial light modulators typically utilized in these correlators has not been experimentally measured. The results of some experiments which show a nonlinear response of the modulated read beam as a function of the write light intensity for the optically addressed ferroelectric LC SLM are presented in this section.

The experimental system shown in Figure 10 was used with the FELC SLM. A HeNe laser was spatially filtered and collimated using standard laboratory techniques. A half-wave plate in conjunction with a mirror and a beam-splitter (BS) was used to effectively divert this beam to the read side of the modulator. A spatially filtered and collimated beam from an Argon ion laser was used as the write beam source. Prior to the polarizing beamsplitter (PBS) in the write beam, a variable beamsplitter (VBS) was inserted to adjust the intensity of the write beam. A half-wave plate in conjunction with the PBS was used to divide the light into two equal intensity beams. One of these beams was used to write to the SLM while the other beam was used to monitor the intensity of the write beam by using an NRC model 815-SL power meter (Detector #1). Furthermore, the read beam reflected from the SLM was imaged into a second NRC power meter (Detector #2).

The modulated read beam was measured for varying write light intensities when the FELC SLM was operated in "maximum contrast" and "phase-only" modes. The maximum contrast state was determined by inserting a USAF resolution chart at plane P. This chart was then imaged onto the write side of the SLM using lens L2, a 50 mm focal length TV imaging lens. The polarizer in the read beam and the driving frequency of the FELC SLM were adjusted to achieve maximum contrast at detector #2. Maximum contrast was qualitatively determined by temporarily replacing the detector with a CCD camera and visually assessing the resultant image. Once maximum contrast was achieved, the resolution chart was removed and the variable beamsplitter was adjusted while write and read beam intensities were measured from detector #1 and detector #2, respectively. The FELC SLM was then adjusted to operate in a "phase-only" mode. This mode was determined by reinserting the resolution chart at plane P and adjusting the polarizer in the read beam until no apparent contrast was evident. Although the contrast of the read beam was minimized, some amplitude modulation was evident in the read beam. The chart was then removed and the write and read beam intensities were recorded for various write light intensities. The results of these "maximum contrast" and "phase-only" measurements are shown in Figure 11.

The results presented graphically in Figure 11 definitively show regions of nonlinear response of the modulated read beam as a function of the write beam intensity. Research is currently being performed to determine the effects of this nonlinearity on the spatial frequencies written to this spatial light modulator. Perhaps the nonlinearity may be utilized to effectively tailor spatial frequency variations for optimal performance of an optical processing architecture. The effects of this nonlinear spatial frequency tailoring on optical correlator architectures are currently being studied.

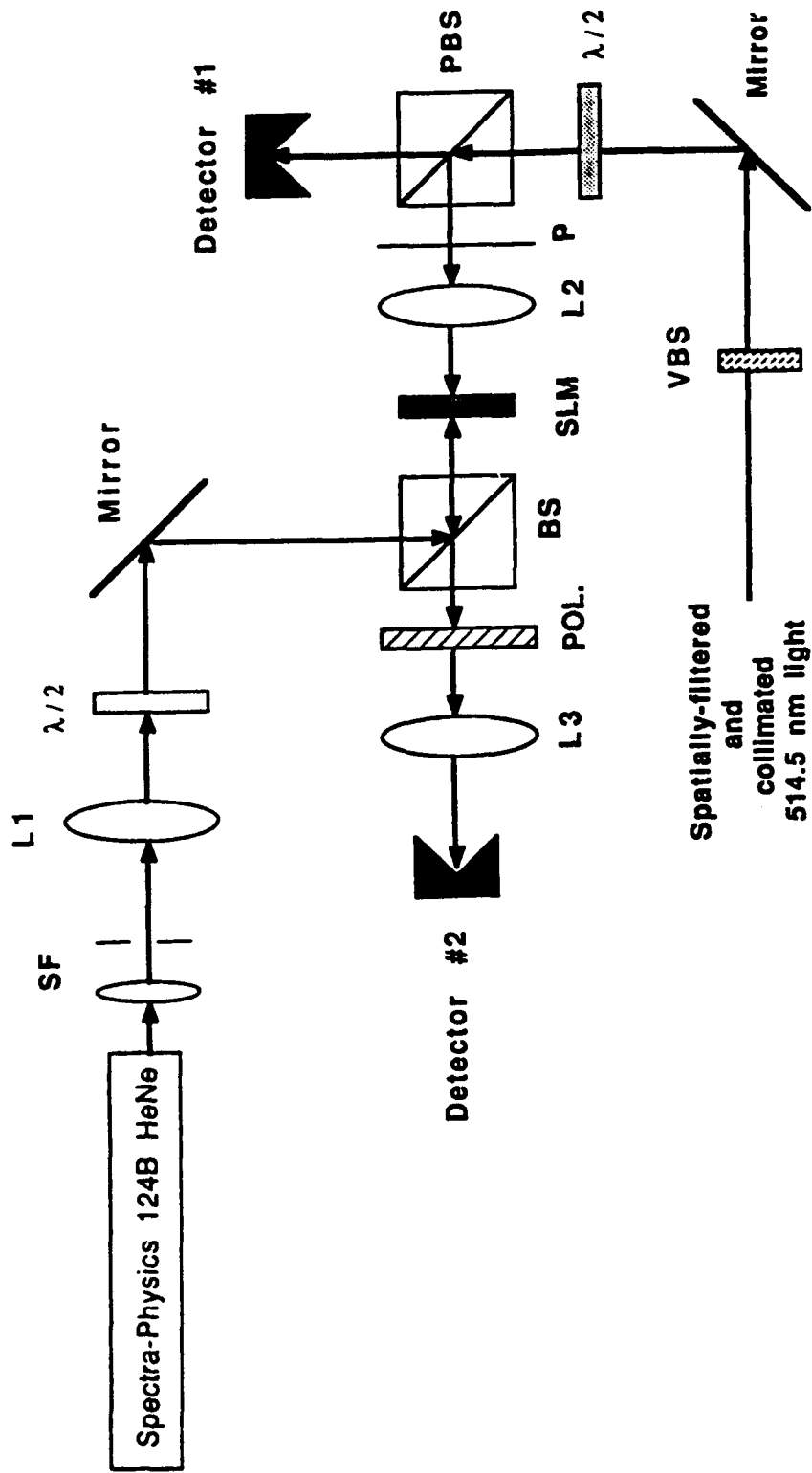
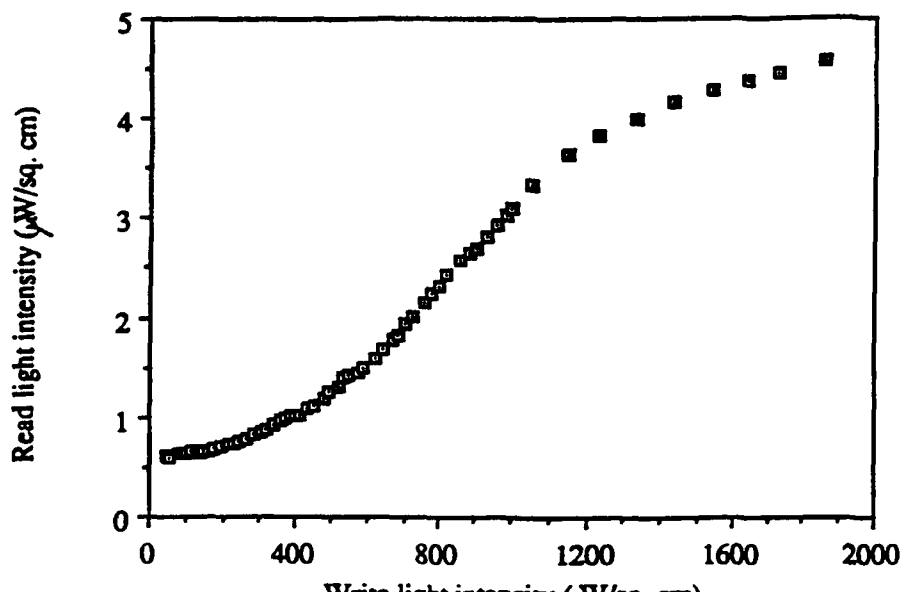
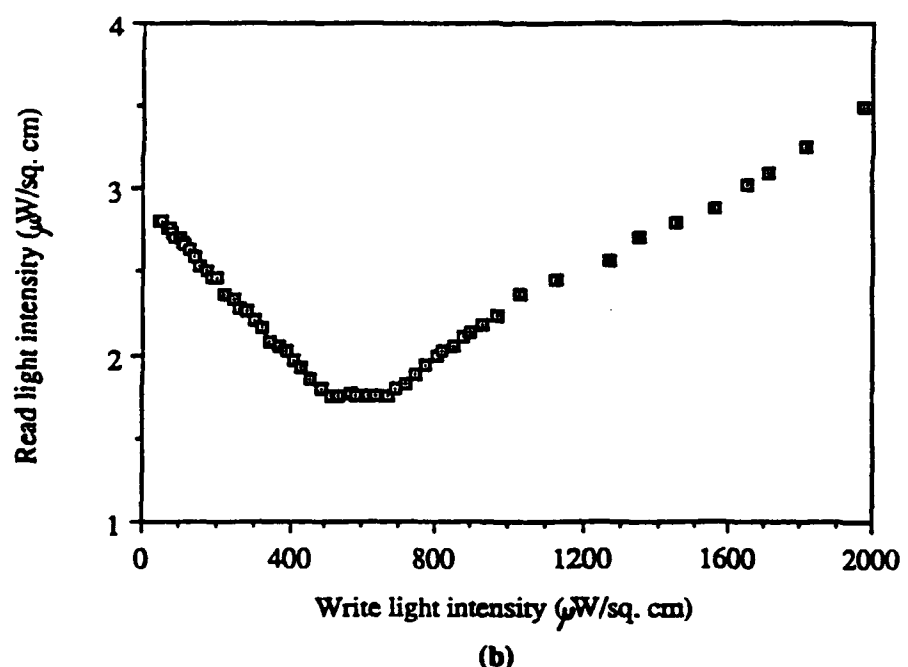


Figure 10. Experimental system used to measure the response of the FELC SLM to variations in write light intensity.



(a)



(b)

Figure 11. The response of the ferroelectric liquid crystal SLM with the device operated in (a) maximum contrast and (b) "phase mostly" mode.

VII. CONCLUSIONS

Several performance characteristics of an optically-addressed ferroelectric spatial light modulator have been experimentally measured. These characteristics include response time, resolution, and visibility. The laboratory grade modulator was able to resolve at least 40 lp/mm at a visibility of 0.9. Furthermore, the device responded to an update of the input image occurring every 17 milliseconds at maximum visibility.

Several modifications are desired in future generations of this modulator. These modifications include the use of a dielectric mirror and optical flats. The dielectric mirror would isolate the read and write beams, thereby reducing the sensitivity of the write light required. The optical flats will minimize or eliminate the Newton's rings formed in the image read from the device. This modification will improve the visibility of the image read from the modulator. It is believed that the above mentioned modifications can be successfully achieved with currently available technology and equipment.

REFERENCES

1. G. Moddel, et. al., "High-Speed Binary Optically Addressed Spatial Light Modulator," *Appl. Phys. Lett.* 55(6), 537-539 (1989).
2. Davis, J. A., Gamlieli, J., and Bach, G. W., "Optical Transmission and Contrast Ratio Studies of the Magneto-Optic Spatial Light Modulator," *Applied Optics* 27(24), 5194-5201 (1988).
3. Gregory, D. A., Juday, R. D., Sampsell, J., Gale, R., Cohn, R. W., and Monroe, S. E., Jr., "Optical Characteristics of a Deformable-Mirror Spatial Light Modulator," *Opt. Ltr.* 13(1), 10-12 (1988).
4. T. Hara, et. al., "Microchannel Spatial Light Modulator Having the Functions of Image Zooming, Shifting, and Rotating," *Appl. Opt.* 25(14), 2306-2310 (1986).
5. Johnson, K. M., Handschy, M. A., and Pagano-Stauffer, L. A., "Optical Computing and Image Processing With Ferroelectric Liquid Crystals," *Opt. Eng.* 26(5), 385-391 (1987).
6. D. Williams, et. al., "An Amorphous Silicon/Chiral Smectic Spatial Light Modulator," *J. Phys. D* 21, S156-S159 (1988).
7. Grinberg, J., Jacobson, A., Bleha, W., Miller, L., Fraas, L., Boswell, D., and Myer, G., "A New Real-Time Non-Coherent to Coherent Light Image Converter-the Hybrid Field Effect Liquid Crystal Light Valve," *Opt. Eng.* 14(3), 217-223 (1975).
8. British Drug House (BDH) Limited, Broom Road, Poole, GH12 4 NN, England.
9. Li, W., Rice, R. A., Moddel, G., Pagano-Stauffer, L. A., and Handschy, M., "Hydrogenated Amorphous-Silicon Photosensor for Optically Addressed High-Speed Spatial Light Modulator," *IEEE Trans. on Electron Devices* 36(12), 2959-2964 (1989).
10. Solymar, L., and Cooke, D. J., Volume Holography and Volume Gratings, Chapter 5.6, pp 127-129, Academic Press, 1981.
11. Max Born and Emil Wolf, Principles of Optics, Sixth Edition, pg. 267, Pergamon Press, New York (1980).
12. R. E. Simon, ed., RCS Electro-Optics Handbook Technical Series EOH-11, pg. 114, RCA Corporation, Harrison, NJ (1974).
13. R. E. Simon, ed., RCA Electro-Optics Handbook Technical Series EOH-11, pg. 117, RCA Corporation, Harrison, NJ (1974).
14. Hawk, James F., "The Suitability of Liquid Crystal Television Receivers for Applications in High Resolution Optical Pattern Recognition," U.S. Army Missile Command Contract No. DAAL03-86-D-0001, Redstone Arsenal, AL, 25 August 1989.

REFERENCES (Concluded)

15. Javidi, B., and Kuo, C. J., "Joint Transform Image Correlation Using a Binary Spatial Light Modulator at the Fourier Plane," *Applied Optics* 27 (1988) 663-665.
16. Javidi, B., and Horner, J. L., "Single SLM Joint Transform Correlator," *Applied Optics* 28 (1989) 2358-2367.
17. Javidi, B., "Nonlinear Joint Power Spectrum Based Optical Correlator," *Applied Optics* 28 (1989) 262-267.
18. Javidi, B., "Nonlinear Matched Filter Based Optical Correlation," *SPIE Proceedings* 1151 (1989) 262-267.
19. Javidi, B., "Generalization of the Linear Matched Filter Concept to Nonlinear Matched Filters," submitted to *Applied Optics*.

DISTRIBUTION

	<u>Copies</u>
Director U.S. Army Research Office ATTN: SLCRO-PH SLCRO-ZC P.O. Box 12211 Research Triangle Park, NC 27709-2211	1 1
Headquarters Department of the Army DAMA-ARR Washington, DC 20310-0632	1
Headquarters OUSDRAE The Pentagon ATTN: Dr. Ted Berlincourt Washington, DC 20310-9632	1
Defense Advanced Research Projects Agency Defense Sciences Office Electronics Systems Division ATTN: Dr. A. Yang 1400 Wilson Boulevard Arlington, VA 22209	1
Commander U.S. Army Foreign Science and Technology Center ATTN: AIAST-RA 220 Seventh Street, N.E. Charlottesville, VA 22901-5396	1
Director, URI University of Rochester College of Engineering and Applied Science The Institute of Optics Rochester, NY 14627	1
Director, JSOP University of Arizona Optical Science Center Tucson, AZ 85721	1
Electro-Optical Terminal Guidance Branch Armament Laboratory ATTN: Dr. Steve Butler Eglin Air Force Base, FL 32542	1

DISTRIBUTION (Continued)

	<u>Copies</u>
U.S. Army Cold Regions Research and Engineering Laboratory ATTN: Dr. Richard Munis 72 Lyme Mill Road Hanover, NH 03755	1
Night Vision and Electro-Optics Center ATTN: AMSEL-NV-T, Mark Norton Building 357 Fort Belvoir, VA 22060	1
RADC/ESOP ATTN: Dr. Joseph Horner Hanscom AFB, MA 01731	1
Applied Science Division Applied Optics Operations ATTN: Mr. Jeff Sloan P.O. Box 3115 Garden Grove, CA 92641	1
Department of Electrical Engineering Stanford University ATTN: Dr. J. W. Goodman Stanford, CA 94305	1
University of Alabama in Huntsville Center for Applied Optics ATTN: Dr. H. John Caulfield Huntsville, AL 35899	1
University of Alabama in Huntsville Physics Department ATTN: Dr. J. G. Duthie Huntsville, AL 35899	1
Carnegie-Mellon University Department of Electrical and Computer Engineering ATTN: Dr. David Cassasent Pittsburgh, PA 14213	1
Penn State University Department of Electrical Engineering ATTN: Dr. F. T. S. Yu University Park, PA 16802	1

DISTRIBUTION (Continued)

	<u>Copies</u>
University of Alabama in Birmingham Physics Department ATTN: Mr. James F. Hawk University Station Birmingham, AL 35294	1
NASA Johnson Space Center ATTN: Code EE-6, Dr. Richard Juday Houston, TX 77058	1
Jet Propulsion Lab ATTN: Dr. Michael Shumate 4800 Oak Grove Drive Pasadena, CA 91109	1
Naval Weapons Center ATTN: Code 3941, David Bloom China Lake, CA 93555	1
University of Colorado at Boulder Department of Electrical and Computer Engineering ATTN: Dr. Kristina Johnson Boulder, CO 80309-0425	1
Naval Research Lab ATTN: Code 6537, Dr. Arthur Fisher Washington, D.C. 20375-5000	1
U.S. Army Materiel System Analysis Activity ATTN: AMXSY-MP (Herbert Cohen) Aberdeen Proving Grounds, MD 21005	1
IIT Research Institute ATTN: GACIAC 10 W. 35th Street Chicago, IL 60616	1
Optical Corp of America - Applied Optics 7421 Orangewood Ave Garden Grove, CA 92641	1

DISTRIBUTION (Concluded)

	<u>Copies</u>
AMSMI-RD	1
-RD-WS, Dr. Bennett	1
-RD-WS-PO, Mr. R. Kevin Worcester	1
Dr. Don A. Gregory	15
Mr. David J. Lanteigne	1
Mr. James C. Kirsch	1
Mr. Tracy D. Hudson	80
AMSMI-RD-CS-R	15
AMSMI-RD-CS-T	1
AMSMI-GC-IP, Mr. Bush	1
DASD-H-V	1